

Diffuse Reflection Infrared Fourier-transform Spectroscopy and Partial Least Squares Regression Analysis for Temperature Prediction of Irreversible Thermo-chromic Paints

Akiharu Kitagawa,¹ Calum Welsh,³ Harry Mackilligin,⁴ Peter Licence*^{1,2}

¹GSK Carbon Neutral Laboratory for Sustainable Chemistry, University of Nottingham, Jubilee Campus, Nottingham NG7 2TU, UK

²School of Chemistry, University of Nottingham, University Park, Nottingham NG7 2RD, UK

³Calum.Welsh@mt.com

⁴Rolls-Royce plc, Thermal Paints Lab, df29, A-Site, Victory Road, DE24 8EN, UK

*email: peter.licence@nottingham.ac.uk; Tel. 0115 846 6176

Abstract

Temperature measurement of internal components of a jet engine is a crucial control parameter to ensure its component life and efficiency. Particularly for thermal analysis of internal components of jet engines, irreversible thermo-chromic paints (TPs) have been developed at Rolls-Royce plc. to evaluate the surface temperature of engine components where it is otherwise impossible. TPs change color with respect to an increased temperature whereby the resulting change in the TP color corresponds to the maximum temperature experienced by the surface of engine components during testing. To improve the reliability and reproducibility of the temperature measurement by TPs, this work explored the potential use of diffuse reflection Fourier-transform infrared spectroscopy (DRIFTS) combined with partial least squares regression (PLSR) analysis. The outcome of the prediction of the raw and pre-processed datasets was compared and discussed. The major contributors to the prediction models were the change in the property of the surface M-OH bonds,

the structural change of the inorganic pigments and fillers, and their solid-state reaction at a higher temperature. The result showed improved reliability of the prediction model after the combined pre-process treatments with reported RMSEC of 4.5 °C and RMSECV of 13.0 °C using 3 latent variables.

Introduction

Temperature measurement control is an important parameter to ensure component life and to improve the performance efficiency of machinery and engines operating at high temperature. To acquire the surface thermal information of turbine jet engine components, irreversible thermochromic paints (TPs) have been developed at Rolls-Royce plc (RR).^{1,2} The surface thermal profile is obtained utilizing temperature-dependent color change, which is mostly due to 1) thermal decomposition of pigments, 2) structural changes of the inorganic pigments and fillers, and 3) high-temperature solid-state reaction of inorganic pigments resulting in new spinel species.³⁻⁶ The series of TPs at RR incorporates various thermochromic pigments such as ultramarine violet ($\text{Al}_6\text{Na}_6\text{O}_{24}\text{S}_{(3-4)}\text{Si}_6$) and cobalt ammonium phosphate, to obtain the most optimal color changes on the applied surface. The surface temperature is determined by applying TP on engine components before an engine test and comparing the changed colors of the surface of disassembled engine components to the calibrated color-temperature reference of TP.

Although the use of TPs provides detailed thermal information of the surfaces of the engine components with a temperature range from 300 to 1200 °C, the performance capability of TP depends on its color change that is examined by the human eye. Hence, there has been a continuous effort to improve the precision of the temperature measurement, where it is currently limited to the visible color change of TP. One approach to refine existing TP technology is the use of non-contact and non-destructive spectroscopic surface analysis techniques. Specifically, temperature

measurement using TP may improve by capturing spectroscopic information outside of the visible spectrum and correlating the chemical information to the temperature at which TP was exposed. The spectral information collected from a sample surface can be analysed with multivariate analysis to highlight the most important spectral information related to the variable factors of interest. The use of chemometrics techniques in combination with spectroscopy, namely diffuse reflection infrared Fourier-transform spectroscopy (DRIFTS), has been widely applied in many fields such as geological analysis, art conservation, and food science to monitor the chemical change of samples to discover otherwise elusive information.⁷⁻¹⁰ Data collection by DRIFTS is also both fast and non-destructive, which is beneficial for inspection and temperature measurement of TPs on post-test engine components.

A widely used data processing method for spectroscopy is partial least squares regression (PLSR). One of the main benefits of PLSR is that it enables correlation of observed information in a dataset with the independent variable(s) to develop a quantitative prediction model. It is a rapid, interpretive method that utilises the most important chemical information from a material of interest, and its statistical analysis allows the user to comprehend the most significant contributing factors to the predicted outcome. The use of DRIFTS combined with chemometrics technique to determine the temperature of TP has never been reported. Therefore, the present work explores the potential application of DRIFTS-PLSR analysis to predict the temperature of a TP after thermal treatment. The raw and pre-processed datasets were compared to improve the prediction model and the statistical information obtained from PLSR was used to interpret the spectral dataset in relation to the thermal behavior of the TP.

Theory

Partial Least Square Analysis

Spectral information is often processed using multivariate analysis to reveal relationships between the sample and changing variables or processing methods. PLSR works by using regression of a dataset whose mathematical process is expressed as:¹¹

$$\mathbf{X} = \mathbf{TP}' + \mathbf{E} \quad (1)$$

where \mathbf{X} is the original matrix of the spectral data, \mathbf{T} and \mathbf{P} are the score values and loading spectrum of a latent variable (LV), or a dimension of the dataset, respectively, and \mathbf{E} is the residual matrix obtained after regression of each LV, which is used as the matrix for the succeeding LV. In spectroscopic applications, \mathbf{T} values are often used to describe the level of similarity or differences of a sample within the whole population. It is a useful value to observe the trends of the collected spectral sample to the developed model. \mathbf{P} is used to determine which component(s) of a spectrum had contributed to the development of a model in each LV.¹² For a further explanation, refer to the paper by Wold, et. al.¹¹

Pre-Processing

To acquire the most relevant information of interest, it is a common practice to treat the dataset with pre-processing algorithms. This step often excludes unwanted information such as baseline shifts and noises to highlight more relevant information, which depends on the physical and chemical nature of the sample as well as the end goal of the analysis. In this work, the following pre-process treatments were applied to maximise the use of chemical information of the TP from the spectra: standard normal variate transformation (SNV), autoscale, and orthogonal signal correction (OSC). These pre-processing were applied in the respective order to the \mathbf{X} -block (spectral data) and the \mathbf{Y} -block (temperature of TP) were mean-centred.

SNV is a process in which the spectra are normalised by the standard deviation of the intensity values at each spectral index, expressed as:

$$SNV_i = \frac{(x_i - \bar{x})}{\sqrt{\frac{\sum(x_i - \bar{x})^2}{n-1}}} \quad (2)$$

Where SNV_i is the transformed intensity value at each i^{th} wavenumber index, x is the original intensity value at i , \bar{x} is the average intensity of all spectra at i , and n is the number of spectra collected. In the context of a spectroscopic application, SNV normalises each spectrum to its standard deviation; each spectrum weighs in equally to the model.¹³

Autoscale was then applied after the SNV treatment. Autoscale is arguably one of the most used pre-processing methods, which mean-centres the dataset and normalises to its new standard deviation:

$$MC_i = x_i - \bar{x}, AC_i = \frac{(x_i - \bar{x})}{\sqrt{\frac{\sum(MC_i - \overline{MC})^2}{n-1}}} \quad (3)$$

where MC_i is the new spectral intensity after the mean-centring process and AC_i is the new spectral intensity after the autoscaling process at each spectral index. The mean-centred spectrum possesses a unique identity within the dataset, and by normalising the spectrum by its standard deviation of mean-centred spectra, the value at all wavenumbers of a spectrum holds equal importance. Ultimately SNV normalises the spectral dataset per spectrum and autoscale per wavenumber.

Finally, orthogonal signal correction (OSC), which is a powerful tool to reduce background noise,¹⁴ was applied to the dataset. After this process, the first LV contains the minimal covariance between the changes in the spectra to increasing temperature, therefore, extracting the maximum correlated spectral information with respect to the increasing temperature. The resulting dataset contains a highly linear relationship between **X**-block and **Y**-block. OSC works in such a way that it finds information of **X** that is orthogonal (unrelated) to the trend of **Y**:

$$\mathbf{T}^* = (1 - \mathbf{Y}(\mathbf{Y}'\mathbf{Y})^{-1}\mathbf{Y}')\mathbf{T} \quad (4)$$

where the \mathbf{T}^* is the updated orthogonal score vector, whose predicted response is calculated in the same manner as PLSER. By applying OSC after SNV and autoscale, which highlights all the important spectral information for prediction, the outcome of the prediction can be improved drastically as compared to the outcome using the raw data.

Statistical Analysis

To evaluate the quality and fitness of the developed model, it is important to evaluate the statistical analysis to determine any outliers, trend, or bias caused by the model development. Q-residuals and Hotelling's T^2 are two reliable statistic values to find data points that could ultimately affect the model quality significantly due to the unique properties of which a data point may contain.¹⁵ Q-residual evaluates the fitness of the data points to the developed model using the residual matrix of each latent variable (LV). An abnormal value of Q-residual of a data point in comparison to the sample population may indicate that the sample may contain a systematic or random error from data collection or pre-processing.

Hotelling's T^2 indicates the fitness of the correlation between samples and the prediction model. Note that, unlike Q-residual statistics, Hottelings' T^2 incorporates the score matrix, \mathbf{T} , that is used to explain the nature and behavior of the samples within the model, rather than evaluating the residual vector of each LV.¹⁵ Ultimately, Hotelling's T^2 describes the variation of the samples within the model. The outcome of the statistical methods above was used to describe the models of raw and pre-processed data and to compare the effect of pre-processing.

Materials and Method

Thermochromic Paint (TP)

Samples of TPs were prepared at Rolls-Royce PLC, Derby, United Kingdom. TP calibration coupons were prepared by cold-spray painting the TP on coupons ($15 \times 25 \times 2$ mm) of Nimonic75, cured at $300\text{ }^{\circ}\text{C}$ for an hour, and left to cool at room temperature for an hour. Each coupon was then heated to the desired temperature in a Thermal Cycling furnace (Carbolite, UK) in the air for 3 minutes. After 3 minutes, the coupon is cooled to room temperature. A set of calibration coupons were prepared in the range of 470 to $1260\text{ }^{\circ}\text{C}$ with $10\text{ }^{\circ}\text{C}$ incrementations. The thickness of the TP layer on the coupons was measured by a PosiTector® 6000 (DeFelsko®, USA), to ensure consistent thickness for all coupons (see Table S1).

A gradual color change of TP was obtained by heating a bowtie-shape Nimonic75 sample with a customized induction heater (Bowyer Engineering, UK). Three bowtie samples were prepared by spray painting the TP onto a bowtie shaped Nimonic75 ($50 \times 180 \times 2$ mm) and the samples were cured at $300\text{ }^{\circ}\text{C}$ for an hour. The bowtie samples were cooled for an hour at room temperature then heated for 3 minutes at the highest temperature of $1200\text{ }^{\circ}\text{C}$ at the narrowest point of the sample where thermocouples were welded. (**Fig 1 & Fig2**). The bowtie samples were used for line-scan measurement to test the prediction model on a surface with gradual and continuous color change.



Fig 1: An image of the bowtie sample painted with TP, prepared as shown by a customized induction heater. The hottest temperature was set to be $1200\text{ }^{\circ}\text{C}$ where the TP turned black. The spectra used for prediction were collected along a straight line in the middle with increments of 5mm.

Diffuse Reflection Infrared Fourier-transform (DRIFT) Spectroscopy

Diffuse reflection infrared Fourier-transform (DRIFT) spectroscopy allows the collection of structural information of the surface of TP in a non-destructive manner with minimal sample preparation. It is also beneficial for analysis of non-smooth surface as the process considers both absorption and scattering of the incident light by the surface using Kubelka-Munk transformation, which is approximately proportional to the absorption spectra:¹⁶

$$\frac{K}{S} = \frac{(1-R_{\infty})^2}{2R_{\infty}} \quad (5)$$

where R_{∞} is the reflection of the surface, which is the ratio of the absorption coefficient, K , and the scattering efficient, S . The IR spectra of the calibration coupons and bowtie samples were collected using ALPHA FT-IR spectrometer (Bruker, Germany) equipped with the UP-DRIFT module (Bruker, Germany). The spectra were obtained in the Kubelka-Munk with atmospheric compensation mode from 400 to 4000 cm^{-1} , with the sample scanning number of 32 and resolution of 4 cm^{-1} . Each spectrum is the average spectrum of three measurements at different locations of the coupon to simulate random sample collection. The line measurement of the bowtie was taken by obtaining a spectrum at every 5 mm in the centre line (**Fig 2**).

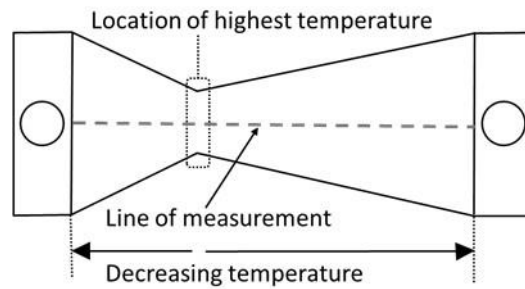


Fig 2: The scheme of the resistance heater testing of a painted bowtie. Thermocouples were welded at the narrowest position of the bowtie (noted as “location of highest temperature”). The temperature decreases toward the edge.

Data processing and PLSR analysis were executed using MATLAB 2017b and its PLSTtoolbox 7.0 by Eigenvector (The MathWorks Inc., USA).

Results and Discussion

Spectroscopic Analysis

To develop a prediction model from spectroscopic data, understanding the original dataset (i.e. the chemical change over increasing temperature) is crucial to optimise the model specifically for the materials of interest. The raw spectra of calibration coupons, which were thermally treated by increments of 10 °C, are presented in **Fig 4a**. In the spectral region above 3000 cm⁻¹, there were two different bands associated with -OH stretching, which were at 3357 cm⁻¹ assigned to the surface M-OH stretching from ultramarine violet, silica, and alumina pigments (**Fig 3b - d**),^{17, 18} and at 3242 cm⁻¹ from -OH group present in the paint resin (**Fig 3e**). The intensity of the M-OH band of the inorganic pigments increased at around 580 °C whereby the maximum intensity was observed at 610 °C and the peak decreased at higher temperatures. This is correlated to the increase of the M-OH bounding site on the surface of the pigments upon heating where the band decreases thereafter due to thermal dehydroxylation.¹⁹ Further, its band maxima position shifted to 3617 cm⁻¹ at around 860 °C, which corresponds to the structural change of alumina pigments leading to altered vibrational activities of Al-OH stretching on the surface.^{17, 20} The M-OH stretch band completely disappears by 980 °C, which is also observed in the corresponding O-H bending peak at 1628 cm⁻¹.

The sharp peaks at 3073, 3052, 2959, 2926, and 2854 cm⁻¹ are attributed to stretching modes of C-H bonds of the resin mixture which burns off by 620 °C. In the same region, there was N-H stretching band from cobalt ammonium phosphate (**Fig 3a**), which overlaps with spectra of the

resin. The impact of the presence of these organic peaks on the prediction model will be discussed later.

After the disappearance of the M-OH bands at around 980 °C inorganic pigments of alumina, silica, and ultramarine pigments show spectroscopic activities of thermal decomposition, solid-state reaction and structural transformation. One of the two most notable peaks is observed in the region of 1200 – 1350 cm⁻¹ after the disappearance of organo-silicone resin. These intense peaks can be assigned to the overlapping of P-O, Si-O-Si, and Si-O-Al bands from the inorganic pigments and fillers, which remain in the TP above 1000 °C.^{19, 21, 22} The peaks remaining at higher temperature are attributed to the silicate glass surface that melted on the coupon surface, which was observed under SEM (see Figure S2).

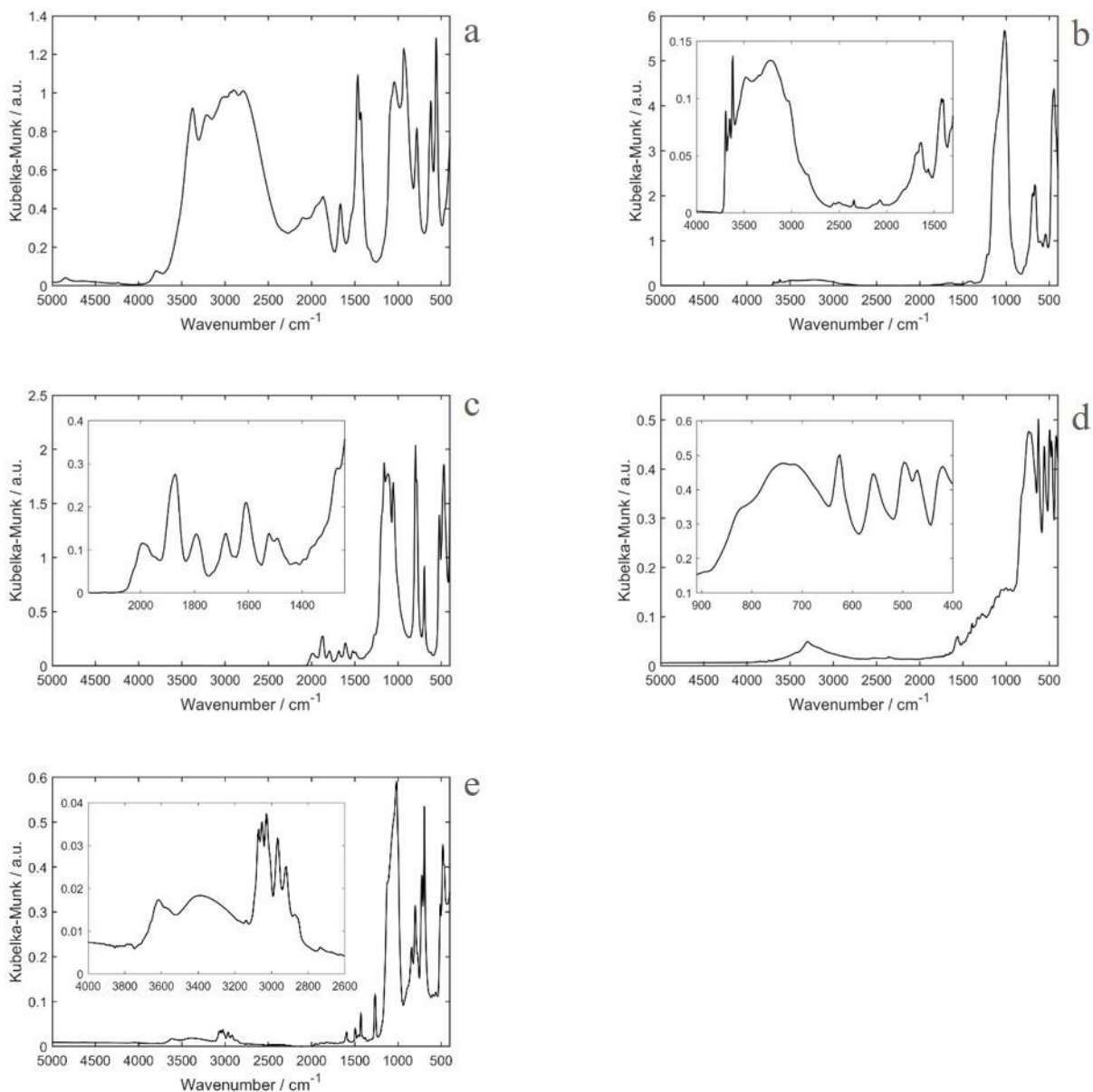


Fig 3: DIRFT spectra of a) cobalt ammonium phosphate; b) ultramarine violet; c) silica; d) alumina; e) paint resin. The materials were not thermally treated. See S1 for measurement parameter.

As described above, the pre-processing method was applied to improve the prediction outcome.

The pre-processed spectra (**Fig 4b**) were difficult to interpret, but some key features were linked back to the raw spectra, such as the change in the M-OH band in the region of 3000 to 3500 cm^{-1} .

It was noted that that the pre-processing method highlighted the shift in the baseline for the samples

treated above 1000 °C. Another strong feature in the pre-processed spectra was the presence of the silica peaks at 1991, 1869, and 1793 cm^{-1} , which was more distinguished in the TP spectra at higher temperature region (> 1100 °C).

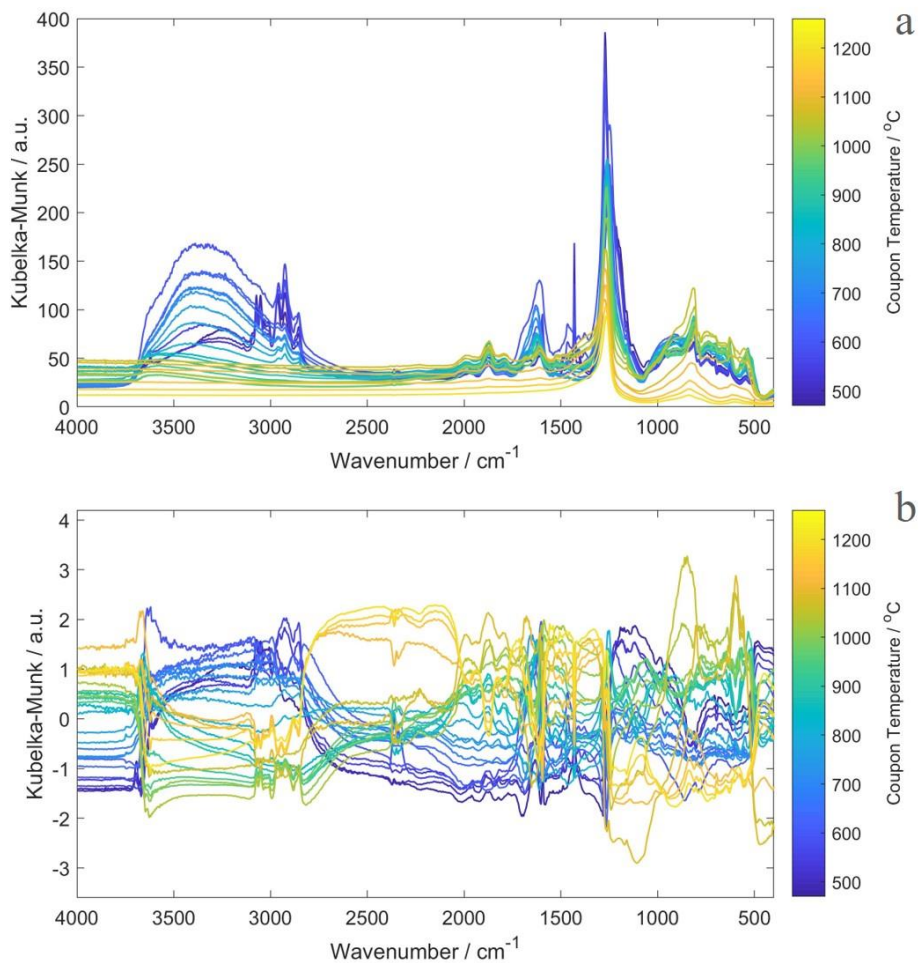


Fig 4: DRIFT spectra of TP collected from UP-DRIFT apparatus. Each presented spectrum was an average of 3 spectra per coupon, and every 3rd spectrum (i.e. temperature increment of 30 °C) is presented for clarity. a) Raw spectra b) Spectra after SN-autoscale-OSC pre-processing treatment.

Temperature Prediction Model Development

After pre-processing, the spectral data were used to create a model to predict the temperature at which the TP has been exposed. The quality of the calibration curve from the pre-processed data

was evaluated by the value of root mean squared error of calibration (RMSEC), which is reported in **Fig5**. 6 LV was used for the model developed with the raw dataset and 3 LV for the model developed with the pre-processed dataset. The developed models were validated using the Venetian blind cross-validation method with the number data splits of 10 and 1 sample per blind. This means that every 10th spectrum was taken out, the model was developed and tested. The RMSEC of the model developed with pre-processed dataset significantly improved, which is 7.3 °C as compared to that of the raw spectra, 48.5 °C. The root mean squared error of cross-validation (RMSECV) was found to be 49.3 °C for the raw data model and 9.07 °C for the pre-processed model. Another notable result was the difference in LV1 Y-block cumulative value of pre-processed data, which was 99.6%, as compared to the raw data, which was 11.9 %. This is the major effect of OSC where the spectral data were orthogonalized to Y-block variable to exclude as much of unrelated spectral data as possible in the first LV, which also resulted in a lower number of LV needed to obtain lower error values, which contributed to the robustness of the model. Lastly, the improvement in the linearity of the calibration curve was especially remarkable in the temperature window above 1100 °C, where very few spectral activities were observed in the raw data.

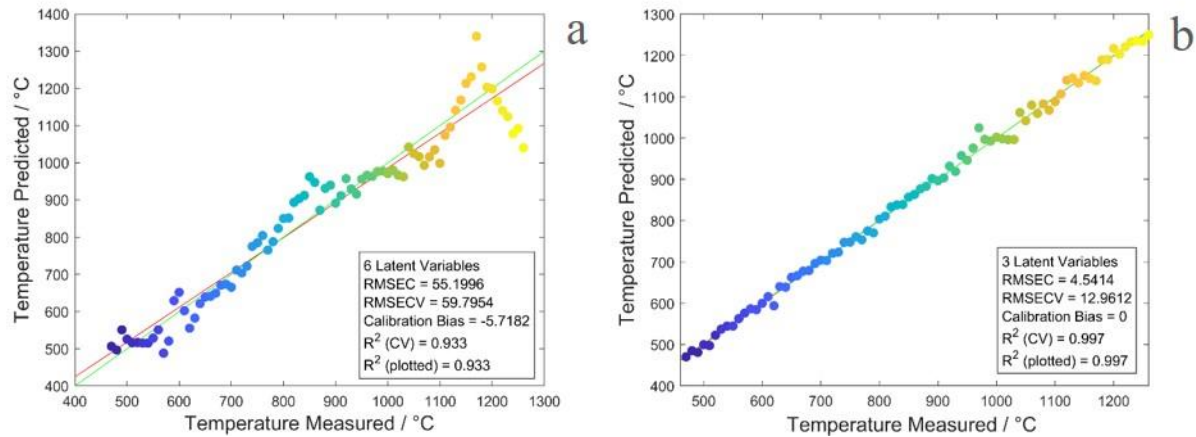


Fig 5: The calibration curves of a) raw spectral dataset and b) pre-processed spectral dataset. Linearity of calibration curves (R^2 values) were reported to be 0.933 and 0.997 for the raw and pre-processed dataset, respectively.

Table 1: The model quality result of the first 5 LVs of the raw and pre-processed data. RMSECV were determined by Venetian-blind cross-validation. Pre-processed data contained 99.6% of Y-block information in LV1, demonstrating the effect of OSC.

LV	X-block LV		X-block Cumulative		Y-block LV		Y-block Cumulative		RMSECV	
	Raw	Pre-process	Raw	Pre-process	Raw	Pre-process	Raw	Pre-process	Raw	Pre-process
1	91.8	49.8	91.8	49.8	11.9	99.6	11.9	99.6	217.2	19.9
2	5.1	31.9	96.9	81.1	59.5	0.3	71.4	99.90	124.0	14.2
3	1.6	8.4	98.5	89.5	13.5	0.06	84.8	99.96	91.1	12.9
4	0.8	2.9	99.3	92.4	3.2	0.01	88.1	99.97	82.5	12.8
5	0.3	3.3	99.6	95.7	3.4	0	91.5	99.97	71.8	12.9

Statistical Analysis

After developing the prediction model, it is important to identify any outliers that may affect the quality of the model and prediction. The Q-residuals and Hotelling's T^2 are two reliable statistic values to determine data points that could be considered as outliers or of which may possess a unique property that ultimately affects the model significantly. In **Fig6a**, the reported Hotelling's T^2 of the pre-processed data show more closely gathered values as compared to the model of the

raw data, except for samples of the spectral from higher temperature coupons. This suggested that after pre-processing, the samples below about 1100 °C were relatively more compatible with the new model than the samples of higher temperature. Similarly, the overall Q-residual values of the pre-processed data decreased, meaning that samples became more fitted to the model itself. As for the robustness of the pre-processed data, it is seen in **Fig6b** and **Fig6d** that the Y-student residual of pre-processed data showed more randomly spread values as compared to the raw data, where the raw data showed a trend in the increasing and decreasing Y-student values in certain temperature windows. The more randomly spread Y-student values of the pre-process data suggested that the data became more prone to the effect of temperature-depended spectral behavior, improving the robustness and fitness of the prediction model.

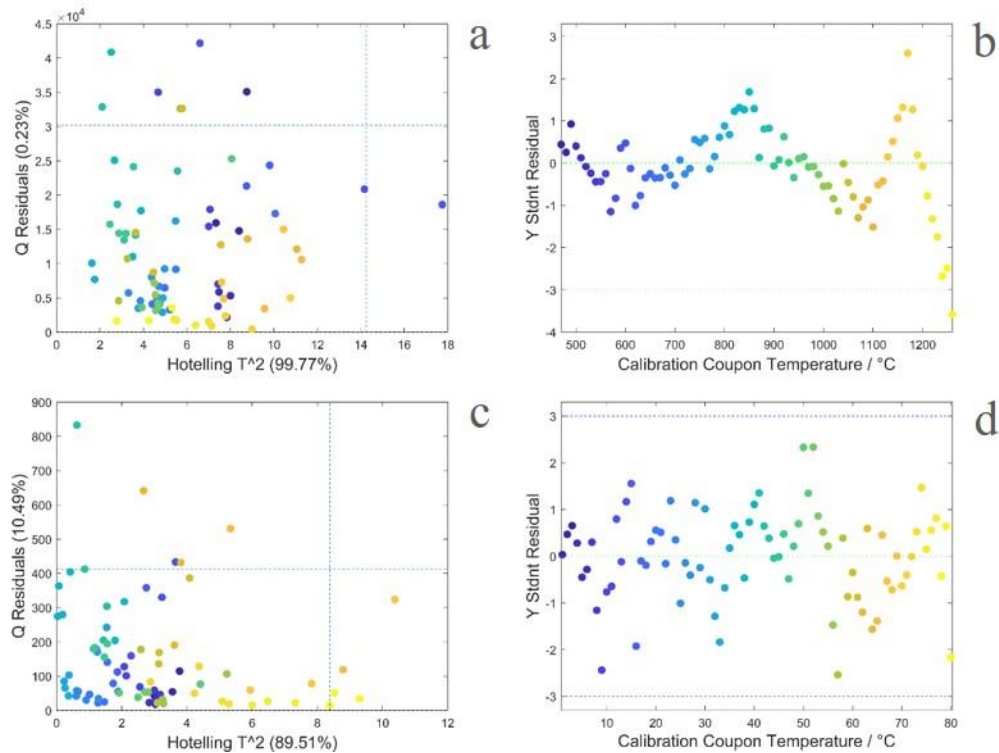


Fig 6: Q residual, Hotelling's T², and Y-student residual values of the raw spectral dataset (a & b) and pre-processed dataset (c & d). The blue dash-lines indicate a 95% confidence level calculated by the software.

Scores and Loadings

Scores and loadings provide a useful insight as the information represent which behavior of the dataset have been captured and used to generate the outcome. For the simplicity of interpretation and comparison, only the scores and loadings of the first three LV are presented. The loading spectra showed the main spectral activities that were correlated to the increasing temperature. In **Fig 7a**, the most notable features were the decrease of the intensities of the (Si-, Al-)OH region of 3357 cm^{-1} and 1620 cm^{-1} , as well as P-O, Si-O-Si, and Si-O-Al region in 1200 cm^{-1} to 1350 cm^{-1} . The same phenomenon was observed in the region below 1000 cm^{-1} where the peak intensity decreases over the temperature window. These activities were positively correlated, which suggested that dehydroxylation and the break down of the silicate-based pigments were the largest contributors to the development of the prediction model. The LV2 (**Fig 7b**) also showed similar spectral behavior, however, the peaks from silica 1991 cm^{-1} , 1869 cm^{-1} , and 1795 cm^{-1} showed a negative correlation relative to the M-OH peak. This suggested that the increase in the silica peak, which was due to the shift of the baseline from the morphology change of the surface at higher temperatures ($>1100\text{ }^{\circ}\text{C}$), had a major contribution to the model development. Likewise, the increase in the intensity at 812 cm^{-1} appeared to have the same effect as it is also negatively correlated to the M-OH peak, whose band intensity decreased over increasing temperature. Lastly, the score and loading spectrum from LV3 (**Fig 7c & f**), which only captured 1.57% of total information, showed the spectral activities of sharp peaks from 2854 cm^{-1} to 3073 cm^{-1} as well as 1430 cm^{-1} that correspond to the organic resin components, whose rapid decomposition was seen between $470\text{ }^{\circ}\text{C}$ to $600\text{ }^{\circ}\text{C}$. Further, the M-OH band in LV3 shows a negative correlation with M-O peaks indicating that LV3 also included the structural change of the inorganic pigments and an

increase in hydroxyl site in the silica, alumina, and ultramarine violet upon heating to around 600 °C.

The score plots and loading spectra of the pre-processed data show significant differences as compared to the raw dataset (**Fig 7g - i**). The most notable difference was seen in the LV1 score plot (**Fig 7j**), which showed great linearity with the increasing temperature of TP, accounting for 99.58% of Y-block. OSC extracted the linear relationship of the given samples and variables, however, applying SN and autoscale before OSC further improved the prediction model. As seen in the LV1 loading plot (**Fig 7g**), the pre-processing treatment highlighted the information of M-OH bands and P-O, Si-O-Si, and Si-O-Al peaks, whose relative intensities were much closer than the raw data. This was the result of the OSC process where the new weight vector was calculated to include the maximum covariance of X-block and Y-block, and the loading showed the most important spectral features of the TP. In **Fig 7k**, LV2 contributed 0.32% to the prediction model where spectral activities were captured in three main temperature windows: 470 °C to 590 °C, 590 °C to 1080 °C, and 1080 °C to 1260. These temperature windows were assigned to the decomposition of the organic resins, M-OH band change and baseline shifting, and the activity of inorganic components in the far spectral region ($< 1000 \text{ cm}^{-1}$), respectively. In LV3, although there were important spectral features observed such as the Si-O peak, the loading spectra modified beyond a comprehensive interpretation.

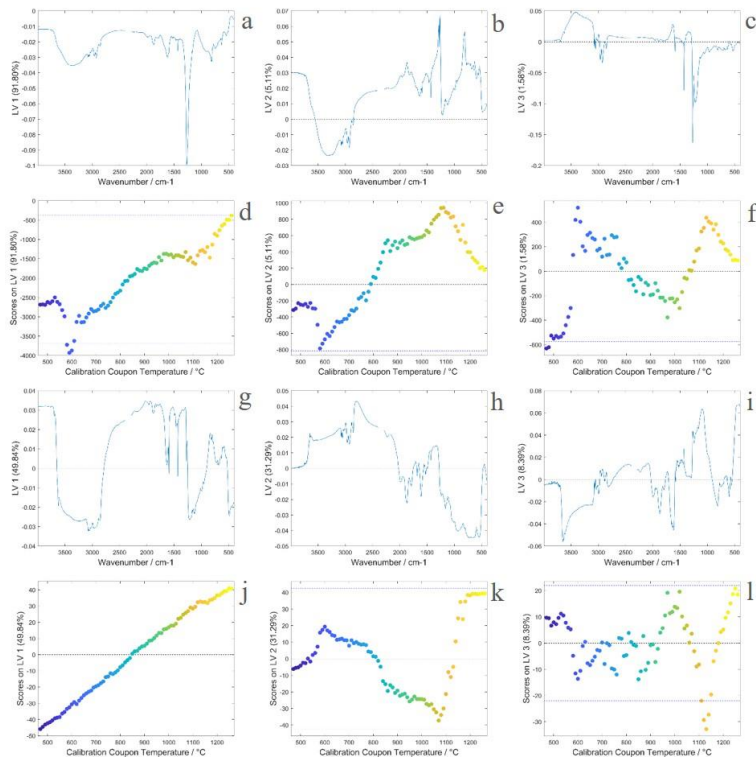


Fig 7: Loadings and score plots of raw (a - f) and pre-processed (g - l) datasets. Only the first three LVs of each dataset were presented for the simplicity of comparison. The spectral region of atmospheric CO₂ was excluded for both models.

Model Testing

To determine the applicability of the model, a separate set of calibration coupons made from a different batch of the same TP were prepared and used for the prediction test. The results are reported in **Table 2**. The comparisons of raw and pre-processed data showed improved prediction outcome by the pre-processed data. The improvement is especially notable in the temperature region of 640 °C to 940 °C where the difference between the treated and predicted temperatures was within 25 °C. This was most likely due to the various spectral activities that took place within this temperature window as previously discussed. However, the prediction model still suffered to produce an accurate outcome for coupons heated at 1140 and 1240 °C, which was probably due to

the lack of spectral activities of the TP temperature at high temperature, which was observed in the unprocessed spectra.

Table 2: The prediction results of the calibration coupons by increments of 100 °C. The presented predicted values were the average of three measurements of the same coupon and standard deviation was calculated from the results of the repeated trial.

Coupon Temperature	Temperature Predicted			
	Raw Data	St. Dev	Pre-processed	St. Dev
540	511.7	6.1	548.8	4.4
640	638.3	8.7	643.9	0.5
740	773.7	2.1	737.1	6.6
840	905.3	17.5	846.9	3.8
940	911.4	18.0	940.8	5.5
1040	1021.8	25.0	1033.1	10.8
1140	1183.4	30.8	1122.9	3.1
1240	1087.9	5.3	1228.7	1.4

The prediction model was further tested on a bowtie substrate heated by the resistance heater up to 1200 °C. The spectra for temperature prediction were collected at every 5 mm of the bowtie, where at 0 and 130 mm were the lowest temperature and 90 to 95 mm was the highest (1200 °C). Through this test, the applicability of the model on the surface with unassigned temperature with a gradual color change was investigated (**Fig8**). First, the result showed an inaccurate outcome in the edges of the bowtie at 0 mm and 130 mm where the predicted temperature was below the curing temperature. This may be due to a high concentration of organic resin components still present on the lower temperature region of the surface, which was seen in the raw spectra of the painted bowtie sample (see Figure S2). The presence of a high concentration of the resin residue contributed to the lowering of the prediction outcome, which must be taken into consideration for the real application. Secondly, the pre-processed data showed three distinct “phases” of temperature change: a sharp change from 0 mm to 20 mm, a gradual change from 20 mm to 60

mm, and another sharp change from 60mm to 95 mm. This may be explained by the LV3 score plot (**Fig 7I**), where the scores of the samples between 700 to 900 °C appeared randomly scattered, hence the prediction outcome was inconsistent in the corresponding region on the bowtie. Although the highest predicted temperature was 1206.9 °C at 85 mm, which was very close to the targeted temperature of 1200 °C, this nonlinear prediction outcome along the bowtie surface indicated that the model still suffered in the region where the spectral information was not fully utilized.

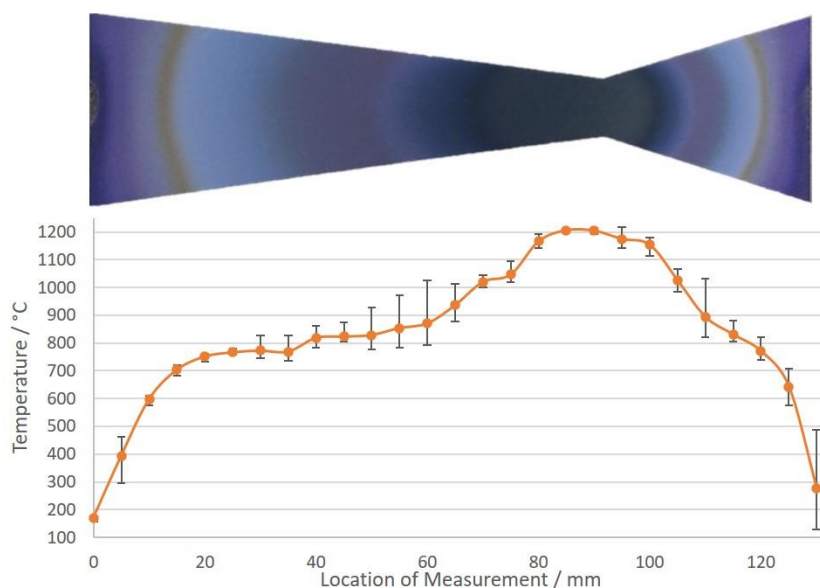


Fig 8: The result from the line measurement temperature prediction of a bowtie sample. The location of measurement at around 90 to 95 mm was the hottest area during the thermal treatment (1200 °C). The points present the average prediction value of three measurements and error bars are the maximum and minimum values of the three trials.

Conclusions

This work demonstrated the interpretation of the temperature prediction model and spectral contribution of the TP that improved the accuracy of the prediction outcome. The prediction model became more robust after pre-processing of the spectral data while the accuracy of prediction drastically improved. Although this was the very first step to explore the potential use of DRIFTS

and PLSR analysis to acquire thermal information of TPs, the results appeared to be promising for further development and application. Advancement in the present work may lead to an automation of temperature reading of TP and the method may be applicable for thermal analysis of other coating materials.

Acknowledgement

We thank EPSRC, (EP/L015633/1, EP/S022236/1 and EP/R025282/1) Rolls-Royce plc, and Thermal Paint Department for support.

Reference

1. E. C. Hodkinson, H. M. L. Watson. Temperature Indicating Paint. US Patent 6673271 B2. Filed 2002. Issued 2004.
2. E. C. Hodkinson, H. M. L. Watson. Temperature Indicating Paint. US Patent 6838286 B2. Filed 2002. Issued 2005.
3. C. Lempereur, R. Andral, J. Y. Prudhomme. "Surface Temperature Measurement on Engine Components by Means of Irreversible Thermal Coatings". *Meas. Sci. Technol.* 2008. 19: 105501
4. Y. Begum, A. J. Wright. "Relating Highly Distorted Jahn–Teller MnO₆ to Colouration in Manganese Violet Pigments". *J. Mater. Chem.* 2012. 22(39): 21110-21116.
5. L. Yang, L. Zhi-min. "The Research of Temperature Indicating Paints and Its Application in Aero-engine Temperature Measurement". *Procedia Eng.* 2015. 99: 1152-1157.
6. E. Lataste, A. Demourgues, J. Salmi, C. Naporea, M. Gaudon, "Thermochromic Behavior (400< T°C<1200°C) of Barium Carbonate/Binary Metal Oxide Mixtures". *Dyes Pigm.* 2011. 91(3): 396-403.
7. M. Manfredi, E. Barberis, A. Rava, E. Robotti, F. Gosetti, E. Marengo. "Portable Diffuse Reflectance Infrared Fourier transform (DRIFT) Technique for the Non-invasive Identification of Canvas Ground: IR Spectra Reference Collection". *Anal. Methods.* 2015, 7(6): 2313-2322.
8. A. Rohman, D. L. Setyaningrum, S. Riyanto. "FTIR Spectroscopy Combined with Partial Least Square for Analysis of Red Fruit Oil in Ternary Mixture System". *Int. J. Spectrosc.* 2014. 2014: 785914.

9. C. Miguel, J. A.Lopes, M. Clarke, M. J. Melo. "Combining Infrared Spectroscopy with Chemometric Analysis for the Characterization of Proteinaceous Binders in Medieval Paints". *Chemon. Intell. Lab. Syst.* 2012. 119: 32-38.
10. M. Ritz, L. Vaculíková, E. Plevová, D. Matýsek, J. Mališ. "Determination of the Predominant Minerals in Sedimentary Rocks by Chemometric Analysis of Infrared Spectra". *Clays Clay Miner.* 2012. 60(6): 655-665.
11. S. Wold, M. Sjöström, L. Eriksson. "PLS-regression: A Basic Tool of Chemometrics". *Chemon. Intell. Lab. Syst.* 2001. 58(2): 109-130.
12. D. M. Haaland, E. V. Thomas. "Partial Least-squares Methods for Spectral Analyses. 1. Relation to Other Quantitative Calibration Methods and the Extraction of Qualitative Information". *Anal. Chem.* 1988. 60(11): 1193-1202.
13. R. J. Barnes. M. S. Dhanoa, S. J. Lister. "Standard Normal Variate Transformation and Detrending of Near-Infrared Diffuse Reflectance Spectra. *Appl. Spectrosc.* 1989. 43(5): 772-777.
14. S. Wold, H. Antti, F. Lindgren, J. Öhman. "Orthogonal Signal Correction of Near-infrared Spectra". *Chemon. Intell. Lab. Syst.* 1998. 44(1): 175-185.
15. L. Mujica, J. Rodellar, A. Fernández, A. Güemes. "Q-statistic and T2-statistic PCA-based Measures for Damage Assessment in Structures". *Struct. Health Monit.* 2011. 10(5): 539-553.
16. V. Džimbeg-Malčić, Z. Barbarić-Mikočević, K. Itrić. "Kubelka-Munk Theory in Describing Optical Properties of Paper (I). *Teh. Vjesn.* 2011. 18(1): 117-124.
17. X. Liu, R. E. Truitt. "DRFT-IR Studies of the Surface of γ -Alumina". *J. Am. Chem. Soc.* 1997. 119(41): 9856-9860.

18. M. Hurukawa, It; Ocirc, S.; ocirc; Kuwahara, T. Preparation of Pigments by Coprecipitation Method (I). Coprecipitation of Aluminum Compounds with Iron (III) Compounds by Sodium Hydroxide". J. Jpn. Soc. Colour Materi. 1976. 49(1): 15-21.
19. K. Byrappa, M. K. Devaraju, P. Madhusudan, A. S. Dayananda, B. V. Suresh Kumar, H. N. Girish, S. Ananda, K. N. Lokanatha Rai, P Javeri. "Synthesis and Characterization of Calcium Aluminum Silicate Hydroxide (CASH) Mineral". J. Mater. Sci. 2006. 41(5): 1395-1398.
20. A. A. Tsyganenko, P. P. Mardilovich. "Structure of Alumina Surfaces". J. Chem. Soc. Faraday Trans. 1996. 92(23): 4843-4852.
21. E. Climent-Pascual, J. R. de Paz, J. Rodríguez-Carvajal, E. Suard, R. Sáez-Puche. "Synthesis and Characterization of the Ultramarine-Type Analog $\text{Na}_{8-x}[\text{Si}_6\text{Al}_6\text{O}_{24}] \cdot (\text{S}_2, \text{S}_3, \text{CO}_3)_{1-2}$ ". Inorg. Chem. 2009. 48(14): 6526-6533.
22. Y. Matsunaga, H. Yamazaki, T. Yokoi, T. Tatsumi, J. Kondo. "IR Characterization of Homogeneously Mixed Silica–Alumina Samples and Dealuminated Y Zeolites by Using Pyridine, CO, and Propene Probe Molecules". J. Phys. Chem. C. 2013. 117: 14043–14050.